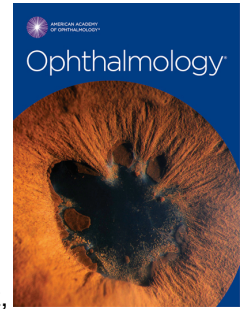


# Journal Pre-proof



Anatomical Changes and Predictors of Angle Widening After Laser Peripheral Iridotomy: The Zhongshan Angle Closure Prevention Trial

Benjamin Y. Xu, MD, PhD, David S. Friedman, MD, PhD, Paul J. Foster, FRCS(Ed), PhD, Yu Jiang, MD, Anmol A. Pardeshi, MS, Yuzhen Jiang, MD, PhD, Beatriz Munoz, MS, Tin Aung, FRCS(Ed), PhD, Mingguang He, MD, PhD

PII: S0161-6420(21)00069-5

DOI: <https://doi.org/10.1016/j.ophtha.2021.01.021>

Reference: OPHTHA 11626

To appear in: *Ophthalmology*

Received Date: 18 November 2020

Revised Date: 30 December 2020

Accepted Date: 19 January 2021

Please cite this article as: Xu BY, Friedman DS, Foster PJ, Jiang Y, Pardeshi AA, Jiang Y, Munoz B, Aung T, He M, Anatomical Changes and Predictors of Angle Widening After Laser Peripheral Iridotomy: The Zhongshan Angle Closure Prevention Trial, *Ophthalmology* (2021), doi: <https://doi.org/10.1016/j.ophtha.2021.01.021>.

This is a PDF file of an article that has undergone enhancements after acceptance, such as the addition of a cover page and metadata, and formatting for readability, but it is not yet the definitive version of record. This version will undergo additional copyediting, typesetting and review before it is published in its final form, but we are providing this version to give early visibility of the article. Please note that, during the production process, errors may be discovered which could affect the content, and all legal disclaimers that apply to the journal pertain.

© 2021 Published by Elsevier Inc. on behalf of the American Academy of Ophthalmology

1 **Anatomical Changes and Predictors of Angle Widening After Laser Peripheral Iridotomy: The**  
2 **Zhongshan Angle Closure Prevention Trial**

3

4 Benjamin Y. Xu, MD, PhD<sup>1</sup>, David S. Friedman, MD, PhD<sup>2</sup>, Paul J. Foster, FRCS(Ed), PhD<sup>3</sup>, Yu Jiang,  
5 MD<sup>4</sup>, Anmol A. Pardeshi, MS<sup>1</sup>, Yuzhen Jiang, MD, PhD<sup>4</sup>, Beatriz Munoz, MS<sup>5</sup>, Tin Aung, FRCS(Ed),  
6 PhD<sup>6</sup>, Mingguang He, MD, PhD<sup>4</sup>

7

8 1. Roski Eye Institute, Keck School of Medicine, University of Southern California, Los Angeles, CA,  
9 USA

10 2. Glaucoma Center of Excellence, Massachusetts Eye and Ear, Harvard University, Boston, MA, USA

11 3. NIHR Biomedical Research Centre at Moorfields Eye Hospital and UCL Institute of Ophthalmology,  
12 London, England

13 4. State Key Laboratory of Ophthalmology, Zhongshan Ophthalmic Center, Sun Yat-sen University,  
14 Guangzhou, People's Republic of China

15 5. Wilmer Eye Institute, Johns Hopkins University, Baltimore, MD, USA

16 6. Singapore Eye Research Institute and Singapore National Eye Centre, Singapore Yong Loo Lin  
17 School of Medicine, National University of Singapore, Singapore

18

19 **Short Title:** Predictors of Angle Widening after Laser Peripheral Iridotomy

20

21 **Corresponding Author:** Benjamin Xu, Department of Ophthalmology, Keck School of Medicine at the  
22 University of Southern California, 1450 San Pablo Street, 4th Floor, Suite 4700, Los Angeles, CA 90033

23 Phone number: 323-442-6780; Fax number: 323-442-6412

24 E-mail: [benjamin.xu@med.usc.edu](mailto:benjamin.xu@med.usc.edu)

25

26

27 **ABSTRACT**

28 **Purpose:** To assess anatomical changes after laser peripheral iridotomy (LPI) and predictors of angle  
29 widening based on anterior segment OCT (AS-OCT) and angle opening based on gonioscopy in mainland  
30 Chinese primary angle closure suspects (PACS).

31 **Design:** Prospective observational study.

32 **Participants:** 454 subjects aged 50 to 70 years with PACS.

33 **Methods:** Subjects received clinical examinations including gonioscopy and AS-OCT imaging at  
34 baseline and 2 weeks after LPI as part of the Zhongshan Angle Closure Prevention (ZAP) Trial. PACS  
35 was defined as inability to visualize pigmented trabecular meshwork in two or more quadrants on static  
36 gonioscopy. LPI was performed on one eye per subject in a superior (between 11 to 1 o'clock) or  
37 temporal or nasal (at or below 10:30 or 1:30 o'clock) location. Biometric parameters in horizontal and  
38 vertical AS-OCT scans were measured and averaged. Multivariable linear and logistic regression  
39 modeling were performed to determine predictors of angle widening, defined as change in continuous  
40 measurements of mean angle opening distance (AOD750), poor angle widening, defined as the lowest  
41 quintile of change in mean AOD750, and poor angle opening, defined as residual PACS after LPI based  
42 on gonioscopy.

43 **Main Outcome Measures:** Anatomical changes and predictors of angle widening and opening after LPI.

44 **Results:** 454 subjects were included in the analysis. 219 received superior LPIs and 235 received  
45 temporal or nasal LPIs. There were significant changes among most biometric parameters ( $p < 0.006$ ) after  
46 LPI, including greater AOD750 ( $p < 0.001$ ). 120 eyes (26.4%) had residual PACS after LPI. In  
47 multivariable regression analysis, several baseline parameters, including superior LPI location ( $p = 0.004$ ),  
48 smaller AOD750 ( $p < 0.001$ ), and greater iris curvature ( $p < 0.001$ ), were predictive of greater angle  
49 widening. Temporal or nasal LPI locations (OR=2.60,  $p < 0.0001$ ) and greater baseline AOD750  
50 (OR=2.58, 0.1 mm increment,  $p < 0.001$ ) were most predictive of poor angle widening based on AS-OCT.  
51 Smaller mean gonioscopy grade (OR=0.34, 1 grade increment) was most predictive of poor angle opening  
52 based on gonioscopy.

53 **Conclusions:** Superior LPI location results in significantly greater angle widening based on AS-OCT  
54 compared to temporal or nasal locations in a Chinese population with PACS. This supports consideration  
55 of superior LPI locations to optimize anatomical changes after LPI.

56

57

58

59

60

61

62

63

64

65

66

67

68

69

70

71

72

73

74

75

76

77

78

## 79 **Introduction**

80 Angle closure, defined as appositional or synechial contact between the trabecular meshwork (TM) and  
81 iris, is the primary risk factor for developing primary angle closure glaucoma (PACG), a leading cause of  
82 permanent vision loss and blindness worldwide.<sup>1,2</sup> Aqueous humor outflow is impaired by angle closure,  
83 which can lead to elevations in intraocular pressure (IOP) and glaucomatous optic neuropathy.<sup>3</sup> There are  
84 effective treatments to alleviate angle closure, including laser peripheral iridotomy (LPI) and lens  
85 extraction surgery.<sup>4</sup> LPI is commonly performed as primary treatment for angle closure as it is safe,  
86 convenient, and produces significant beneficial anatomical changes, including angle widening based on  
87 anterior segment OCT (AS-OCT) imaging and resolution of angle closure based on gonioscopy.<sup>5-9</sup>

88 There is currently no widely-held consensus regarding the optimal location to place an LPI. For  
89 some eyecare providers, LPI location is motivated by the presence and location of iris crypts, which are  
90 localized areas of iris thinning in the anterior-border layer of the iris.<sup>10</sup> For others, LPI location is  
91 motivated by the risk of new-onset dysphotopsias. Traditionally, LPIs were preferentially placed  
92 superiorly beneath the upper eyelid to avoid causing dysphotopsias. Recent evidence suggests that  
93 temporal and nasal LPI locations may actually result in lower incidence of dysphotopsias, although these  
94 findings have not been firmly corroborated.<sup>11-13</sup> One important motivating factor that has not been studied  
95 is the relationship between LPI location and anatomical changes after LPI, even though creating angle  
96 widening and alleviating angle closure are among the primary objectives for performing LPIs.

97 While LPI remains the primary form of treatment for angle closure, recent landmark studies such  
98 as the Effectiveness in Angle-Closure Glaucoma of Lens Extraction (EAGLE) and Zhongshan Angle  
99 Closure Prevention (ZAP) Trials have proposed performing fewer LPIs in specific patient cohorts.<sup>4,14</sup>  
100 Therefore, advancing knowledge about predictors of poor anatomical outcomes after LPI could help  
101 eyecare providers identify patients who should be considered for alternative forms of management, such  
102 as monitoring or lens extraction surgery. In this study, we characterize anatomical changes after LPI in  
103 primary angle closure suspects (PACS) from the ZAP Trial. We also develop statistical models to study

104 the role of baseline parameters, including LPI location and biometric measurements, as predictors of  
105 angle widening based on AS-OCT and angle opening based on gonioscopy after LPI.

106

## 107 **Methods**

108 The ZAP Trial was approved by the Ethical Review Board of Sun Yat Sen University, the Ethical  
109 Committee of Zhongshan Ophthalmic Center, and the Moorfields Eye Hospital and Johns Hopkins  
110 University institutional review boards. Ethics committee approval for the current study was also obtained  
111 from the University of Southern California Medical Center Institutional Review Board. All study  
112 procedures adhered to the recommendations of the Declaration of Helsinki. All study participants  
113 provided informed consent at the time of enrollment.

114

## 115 *Clinical Assessment*

116 Subjects for the current study were identified from the Zhongshan Angle Closure Prevention (ZAP) Trial,  
117 a single-center randomized controlled trial based in Guangzhou, China.<sup>15</sup> Eligible subjects aged 50–70  
118 years with bilateral PACS received complete eye examinations, including gonioscopy and AS-OCT  
119 imaging, by trained ophthalmologists at baseline and 2 weeks after LPI. PACS was defined as an eye with  
120 two or more quadrants of angle closure, defined as inability to visualize pigmented TM based on  
121 gonioscopy, in the absence of peripheral anterior synechiae (PAS), IOP greater than 21 mmHg, and  
122 evidence of glaucomatous optic neuropathy or anterior segment ischemia from previous acute IOP  
123 increase.

124         Static gonioscopy was performed under dark ambient lighting standardized at less than 1 lux  
125 illumination (EA30 EasyView Light Meter; Extech Instruments, Waltham, MA, USA) with a 1-mm light  
126 beam and a Goldmann-type 1-mirror gonioscope (Haag-Streit AG, Koniz, Switzerland) prior to pupillary  
127 dilation. Gonioscopy was performed by one of two fellowship-trained glaucoma specialists with high  
128 intergrader agreement (weighted kappa > 0.80).<sup>15</sup> Care was taken to avoid light falling on the pupil,  
129 inadvertent indentation of the globe, and tilting of the lens greater than 10 degrees. The angle was graded

130 in each quadrant according to the modified Shaffer classification system: grade 0, no structures visible;  
131 grade 1, non-pigmented TM visible; grade 2; pigmented TM visible; grade 3, scleral spur visible; grade 4,  
132 ciliary body visible.

133 AS-OCT imaging was performed with the Visante AS-OCT system (Carl Zeiss Meditec, Inc.,  
134 Dublin, CA, USA) under dark ambient lighting standardized at less than 1 lux illumination prior to  
135 pupillary dilation. During imaging, eyelids were gently retracted taking care to avoid inadvertent pressure  
136 on the globe. At the start of the ZAP Trial, only scans along the horizontal (temporal-nasal) meridian  
137 were performed. Partway through the ZAP Trial, scans along the vertical (superior-inferior) meridian  
138 were also performed.

139 All eligible ZAP subjects received LPI in one eye selected at random using a pre-generated list of  
140 random numbers. LPI was performed on the day of the baseline exam by a trained ophthalmologist using  
141 an Abraham lens (Ocular Instruments, Bellevue, WA, USA) following a standard clinical protocol. A  
142 YAG laser machine (Visulas YAG III, Carl Zeiss Meditec, Dublin, CA, USA) was used to create an  
143 iridotomy starting with an initial setting of 1.5 mJ and titrating as needed to create a patent iridotomy of at  
144 least 200  $\mu\text{m}$  in diameter. LPIs were preferentially placed beneath the superior eyelid unless there was a  
145 prominent iris crypt in a more temporal or nasal location. LPI location was not randomized.

146 Inclusion criteria for the current study included subjects who received gonioscopy and AS-OCT  
147 imaging at baseline and 2 weeks after LPI. Exclusion criteria included eyes missing horizontal or vertical  
148 AS-OCT images.

149

### 150 *AS-OCT Image Analysis*

151 One or two AS-OCT images per eye oriented along the horizontal and/or vertical meridians were  
152 analyzed using custom software (the Zhongshan Angle Assessment Program), which automatically  
153 segmented anterior segment structures and produced biometric measurements once the scleral spurs were  
154 marked.<sup>16</sup> Image analysis was performed by 5 certified graders who were masked to examination results  
155 and intervention assignments. Graders confirmed the segmentation and marked the scleral spurs in each

156 image. The scleral spur was defined as the inward protrusion of the sclera where a change in curvature of  
157 the corneoscleral junction was observed.<sup>17</sup> A set of 20 images from 20 eyes were randomly selected and  
158 graded by all 5 graders independently. Good to excellent inter-grader agreement was evidenced by high  
159 intraclass correlation coefficients (ICC = 0.74-1.00) among all parameters.

160 In total, 13 biometric parameters describing the anterior segment were measured.<sup>18</sup> AOD500 and  
161 AOD750 were defined as the perpendicular distance from the TM at 500 and 750  $\mu\text{m}$  anterior to the  
162 scleral spur to the anterior iris surface, respectively. TISA500 and TISA750 were defined as the areas  
163 bounded anteriorly by AOD500 and AOD750, respectively; posteriorly by a line drawn from the scleral  
164 spur perpendicular to the plane of the inner scleral wall to the opposing iris; superiorly by the inner  
165 corneoscleral wall; and inferiorly by the iris surface. Iris thickness at 750 and 2000  $\mu\text{m}$  from the scleral  
166 spur (IT750 and IT2000), iris area (IA), iris curvature (IC), lens vault (LV), anterior chamber depth  
167 (ACD), anterior chamber width (ACW), anterior chamber area (ACA), and pupillary diameter (PD) were  
168 also measured.<sup>18,19</sup> Eyes with one or more images in which the scleral spur was not detectable or with at  
169 least one missing measurement among the biometric parameters analyzed were excluded from further  
170 analysis.

171

### 172 *Statistical Analysis*

173 Mean parameter measurements were calculated by averaging all sectoral measurements from both  
174 horizontal and vertical images. Anatomical changes after LPI were calculated by subtracting pre-LPI  
175 mean parameter measurements from post-LPI mean parameter measurements. Normality of pre- and post-  
176 LPI parameter measurements was assessed using the Kolmogorov-Smirnov test. All distributions were  
177 non-normal, and pre- and post-LPI parameter measurements were compared using the Wilcoxon signed-  
178 rank test. Change in mean AOD750 after LPI was compared between superior and temporal or nasal LPI  
179 locations using the Wilcoxon rank sum test. Frequencies of poor angle widening and poor angle opening  
180 after LPI were compared between superior and temporal or nasal LPI locations using the chi-square test.



181 Age- and sex- adjusted univariable linear regression analysis was performed to assess the  
182 relationship between baseline parameters and change in mean AOD750 after LPI in  $\mu\text{m}$ . AOD750 was  
183 selected as the outcome measure due to its strong association with gonioscopic angle closure and to  
184 compare our findings to previous studies.<sup>6,20</sup> Spearman correlation coefficients were calculated to assess  
185 for collinearity among biometric parameters. AOD500, TISA500, and TISA750 ( $r > 0.76$  with AOD750),  
186 ACA ( $r = 0.94$  with ACD), and IT2000 ( $r > 0.79$  with IT750) were excluded from multivariable stepwise  
187 models due to high collinearity with other parameters and to maintain variance inflation factors (VIF) less  
188 than 3.0.

189 Multivariable stepwise models based on optimization of the Akaike Information Criteria (AIC)  
190 were developed with the remaining parameters while adjusting for age, sex, and change in PD after LPI.  
191 Units for biometric parameters were modified for physiologic significance and interpretability of beta  
192 coefficients and odds ratios. Multivariable linear and logistic regression modeling were performed to  
193 determine predictors of angle widening, defined as change in continuous measurements of mean  
194 AOD750, poor angle widening, defined as the lowest quintile (20%) of change in mean AOD750, and  
195 poor angle opening, defined as residual PACS (two or more quadrants of angle closure) based on  
196 gonioscopy after LPI. All analyses were performed using the R programming interface (version 4.0.2).  
197 Statistical analyses were conducted using a significance level of 0.05.

198

## 199 **Results**

200 In total, 918 subjects received LPI and clinical examinations, including gonioscopy and AS-OCT  
201 imaging, at baseline and 2 weeks after LPI. 238 subjects (25.9%) were excluded due to missing vertical  
202 images, which were not collected until partway through the ZAP Trial. 37 subjects (4.0%) were excluded  
203 due to missing horizontal images. 189 subjects (20.6%) were excluded due to at least one missing  
204 measurement among the biometric parameters analyzed.

205 454 eyes of 454 subjects were included in the current study. All AS-OCT images from these eyes  
206 had detectable scleral spurs and measurements for all biometric parameters. The mean age of subjects

207 included in the study was  $58.2 \pm 4.7$  years (range 50-69 years). 73 subjects (16.1%) were male and 381  
208 subjects (83.9%) were female, which was consistent with the overall distribution of the ZAP Trial (17%  
209 male, 83% female).<sup>14</sup> All 454 subjects (100.0%) had PACS at baseline prior to LPI. 120 subjects (26.4%)  
210 had residual PACS at 2 weeks after LPI. The mean modified Shaffer grade was  $0.85 \pm 0.58$  at baseline  
211 and  $1.12 \pm 0.78$  at 2 weeks after LPI. 219 subjects received LPIs in superior locations (between 11:00 to  
212 1:00 o'clock) and 235 subjects received LPIs in temporal or nasal locations (at or below 10:30 or 1:30  
213 o'clock).

214 There was a significant difference ( $p < 0.006$ ) between baseline and 2-week measurements for all  
215 biometric parameters except IT2000 ( $p = 0.11$ ) (Table 1). There were significant increases ( $p < 0.006$ ) in  
216 AOD500, AOD750, TISA500, TISA750, IT750, ACD, ACW, ACA, and LV and significant decreases ( $p$   
217  $< 0.001$ ) in IA, IC, and PD at 2 weeks after LPI.

218 There was a significant difference ( $p = 0.03$ ) in the median change in mean AOD750 after LPI  
219 between eyes receiving LPI in superior ( $84.3 \pm 51.8 \mu\text{m}$ ) and temporal or nasal ( $73.4 \pm 52.6 \mu\text{m}$ )  
220 locations. There was a significant difference ( $p = 0.002$ ) in the frequency of eyes with poor angle  
221 widening between superior (31 out of 219; 14.2%) and temporal or nasal (61 out of 235; 26.0%) LPI  
222 locations. There was no significant difference ( $p = 0.69$ ) in the frequency of eyes with poor angle opening  
223 between superior (56 out of 219; 25.6%) and temporal or nasal (64 out of 235; 27.2%) LPI locations.

224 On univariable linear regression analysis, there was a significant association ( $p < 0.05$ ) between 7  
225 baseline parameters and change in AOD750 after LPI after adjusting for age and sex (Table 2). Temporal  
226 or nasal LPI locations were associated with smaller change in AOD750 ( $\beta = -11.09$ ,  $p = 0.025$ ). Greater  
227 AOD750, IC, ACD, ACA, and LV and smaller IT750 and PD were also associated with smaller change in  
228 AOD750 ( $p \leq 0.001$ ). Greater change in PD and smaller change in AOD750 after LPI were significantly  
229 associated ( $\beta = -1.72$ ,  $p = 0.004$ ). There was no association ( $p > 0.29$ ) between age or sex and change in  
230 AOD750 after adjusting for sex and age, respectively.

231 On multivariable linear regression analysis assessing predictors of angle widening after LPI  
232 (overall model adjusted  $R^2 = 0.24$ ), there was a significant association ( $p < 0.01$ ) between 6 baseline

233 parameters and change in AOD750 after LPI after adjusting for age, sex, and change in PD (Table 2).  
234 Temporal or nasal LPI locations were associated with smaller change in AOD750 ( $\beta = -12.81$ ,  $p = 0.004$ ).  
235 Greater AOD750, IA, and PD and smaller IC and ACD were also significantly associated ( $p < 0.01$ ) with  
236 smaller change in AOD750.

237 On multivariable logistic regression analysis assessing predictors of poor angle widening after  
238 LPI (overall model pseudo  $R^2 = 0.18$ ), 5 baseline parameters significantly predicted poor angle widening  
239 after adjusting for age, sex, and change in PD (Table 3). Temporal or nasal LPI locations were associated  
240 with higher odds of poor angle widening (OR = 2.60,  $p < 0.001$ ). Greater AOD750 (OR = 2.58, 0.1 mm  
241 increment), IA (OR = 1.35, 0.1 mm<sup>2</sup> increment), and PD (OR = 1.13, 0.1 mm increment) were also  
242 associated with higher odds of poor angle widening ( $p < 0.001$ ). Greater IC was significantly associated  
243 with lower odds (OR = 0.40, 0.1 mm increment,  $p < 0.001$ ) of poor angle widening.

244 On multivariable logistic regression analysis (overall model pseudo  $R^2 = 0.08$ ), 3 baseline  
245 parameters significantly predicted poor angle opening, after adjusting for age, sex, and change in PD  
246 (Table 4). Greater IA (OR = 1.209, 0.1 mm<sup>2</sup> increment) was associated with higher odds of poor angle  
247 opening ( $p < 0.006$ ). Greater IC (OR = 0.54, 0.1 mm increment,  $p < 0.001$ ) and mean gonioscopy grade  
248 (OR = 0.34, 1 modified Shaffer grade,  $p = 0.001$ ) were associated with lower odds of poor angle opening.

249 There were significant differences between baseline measurements of ACD (2.25 mm for  
250 superior LPI location, 2.21 mm for temporal or nasal LPI locations;  $p = 0.024$ ) and ACA (16.14 mm<sup>2</sup> for  
251 superior location, 15.75 mm<sup>2</sup> for temporal or nasal locations;  $p = 0.039$ ) by LPI location (Table 5). There  
252 were no significant differences ( $p > 0.065$ ) among other baseline parameters, including age and sex.

253

## 254 Discussion

255 We found significant anatomical changes after LPI, including increased angle width based on AS-OCT  
256 and decreased prevalence of PACS based on gonioscopy after LPI in a cohort of mainland Chinese with  
257 PACS. Univariable and multivariable models revealed that angle widening is significantly associated with  
258 not only baseline biometric parameters, such as AOD750 and iris curvature, but also LPI location.

259 Temporal or nasal LPI locations were also strongly predictive of poor angle widening based on AS-OCT,  
260 although they were not predictive of angle opening based on gonioscopy. These results provide the first  
261 evidence of an anatomical benefit to performing LPIs in superior iris locations, which may support  
262 reconsideration of current practice patterns and provide insights into increasing the efficacy of LPI  
263 treatment in angle closure eyes.

264 LPI prevents acute angle closure attacks and at times lowers IOP, especially when IOP is  
265 elevated.<sup>4,14</sup> We hypothesize that it is angle widening after LPI that reduces the likelihood of developing  
266 PAS and elevations in IOP over time. Currently, location of iris crypts and concern for new-onset  
267 dysphotopsias after LPI are the two primary motivating factors for selecting a location for LPI. Our  
268 results suggest that superior LPI locations centered between 11 to 1:00 o'clock provide greater angle  
269 widening than temporal or nasal locations. In our multivariable linear regression model, superior LPI  
270 location resulted in 12.8  $\mu\text{m}$  greater increase in mean AOD750 on average compared to temporal or nasal  
271 LPI locations, which amounts to 16.3% of the 77.7  $\mu\text{m}$  of angle widening observed on average after LPI  
272 in any location. In addition, based on our multivariable logistic regression model, the odds of poor angle  
273 widening after LPI increases by 2.6 times with temporal or nasal LPI locations compared to superior LPI  
274 location. We believe these results support consideration of superior LPI locations to optimize anatomical  
275 changes after LPI.

276 The explanation for the benefit of superior LPI locations is less apparent than the anatomical  
277 benefits. One possible explanation is that the average angle is narrowest superiorly, which makes the  
278 superior sector more likely to respond to LPI.<sup>21,22</sup> However, little is known about the localized or sectoral  
279 effects of LPI treatment and whether angle widening occurs predominantly in the sector in which the LPI  
280 is performed. An alternative explanation is that a superior LPI is more effective at reestablishing aqueous  
281 flow and reducing the pressure gradient between the anterior and posterior chambers, although why this  
282 would be the case is difficult to postulate. Finally, an LPI that is clearly visible in an AS-OCT image may  
283 introduce localized anatomical changes (e.g. iris strands, stromal deformations, PAS) and biases when  
284 measuring biometric parameters. However, there was a visible LPI in only one horizontal (temporal-

285 nasal) image of one subject, which, when removed from the analyses, did not affect our findings.  
286 Therefore, further work is required to elucidate the mechanisms by which superior LPI locations produce  
287 more effective angle widening after LPI.

288 Anatomical changes after LPI are well-characterized and our results based on data from the ZAP  
289 Trial are in agreement with previously reported findings.<sup>5-9</sup> On average, all parameters describing angle  
290 width increased after LPI. In addition, IC decreased, indicating flattening of the convex iris and reduction  
291 of pupillary block. Conversely, LV increased, which may be related to equilibration of pressures in the  
292 anterior and posterior chambers.<sup>6,23</sup> Interestingly, PD decreased after LPI despite carefully controlled  
293 lighting conditions during AS-OCT imaging. This finding may be related to flattening of the iris or  
294 reduction of appositional forces between the iris and lens at their point of contact after LPI.<sup>24</sup> While there  
295 were also significant changes in IT750, IT2000, IA, and ACD after LPI, these changes are likely  
296 statistically but not physiologically significant given their small magnitude and the relatively large study  
297 sample size.

298 The results of our multivariable model of baseline predictors of angle widening, defined by  
299 continuous measurements of AOD750, are also consistent with previous studies.<sup>6,25</sup> Greater mean angle  
300 width at baseline is associated with smaller angle widening after LPI. This is logical, since LPI primarily  
301 treats pupillary block, which likely plays a smaller role in PACS eyes with wider angles. Greater IA and  
302 PD are also associated with smaller angle widening after LPI, presumably due to residual iris tissue  
303 crowding the angle even after LPI. Greater IC is strongly associated with greater angle widening, which  
304 reflects the role of IC as a marker of pupillary block.<sup>26</sup> Greater ACD is also associated with greater angle  
305 widening, presumably because it suggests against a lens-related phacomorphic etiology underlying the  
306 angle closure. Finally, we included change in PD in all models to control for differences in PD between  
307 examinations at baseline and 2 weeks after LPI. The significant association between change in PD and  
308 AOD750 is a reminder that pupil size is a key determinant of angle width and should be controlled or  
309 adjusted for when performing quantitative analyses of angle width across multiple imaging sessions, even  
310 when lighting conditions are carefully controlled.<sup>27,28</sup>

311 Gonioscopy remains the clinical standard for detecting angle closure and forms the basis for  
312 current definitions of primary angle closure disease (PACD).<sup>29</sup> In our study, the majority of LPI-treated  
313 eyes (26.4%) had open angles based on gonioscopy after LPI, consistent with previous studies.<sup>6</sup> In  
314 addition, smaller baseline mean modified Shaffer grade was predictive of poor angle opening after LPI,  
315 which is consistent with previous findings.<sup>6</sup> However, this result stands in contrast to smaller baseline  
316 mean AOD750 predicting greater angle widening. In addition, neither LPI location nor baseline mean  
317 AOD750 were predictive of angle opening based on gonioscopy. These differences among predictors of  
318 angle widening based on AS-OCT and angle opening based on gonioscopy serve as an important  
319 reminder of fundamental differences between AS-OCT and gonioscopic angle assessments, especially in  
320 angle closure eyes.<sup>30,31</sup>

321 We assessed anatomical effects of LPI using horizontal and vertical AS-OCT scans, which is an  
322 important strength of our study. There is significant sectoral variation among biometric measurements,  
323 and analyzing a single horizontal image could miss or misrepresent localized effects of LPI on mean  
324 angle width.<sup>22</sup> However, the increased anatomical accuracy conferred by analyzing more images may also  
325 come at a cost, since each parameter measurements reflects the contributions of a greater number of  
326 localized anatomical features. This may explain why the R-squared metric of our multivariable model of  
327 angle widening ( $R^2 = 0.24$ ) was less than that of a previously reported model ( $R^2 = 0.34$ ), despite  
328 analyzing similar biometric parameters.

329 Our study has some limitations. First, LPI location was not randomized; LPIs were preferentially  
330 placed beneath the superior eyelid unless there was a convenient iris crypt elsewhere. Therefore, iris crypt  
331 status may be a confounder in the relationship between LPI location and angle widening after LPI. That  
332 said, there is no evidence to suggest that performing an LPI at the site of an iris crypt should mitigate its  
333 angle-widening effect. In addition, there were few differences among baseline parameter measurements  
334 when grouped by LPI location, and the greater mean ACD and ACA measurements observed in the  
335 superior LPI group would be expected to decrease rather than increase the apparent angle-widening effect  
336 based on our multivariable linear regression model. Second, all subjects had PACS. Therefore, our results

337 may not generalize to patients with primary angle closure (PAC) and PACG. However, no differences  
338 were observed in the effect of LPI in PACS and PAC/PACG eyes in a previous study, which suggests that  
339 there may not be differences in anatomical changes after LPI based on disease status.<sup>6</sup> Third, all subjects  
340 in the ZAP Trial were Chinese, which again may limit the generalizability of our results. However, there  
341 are many similarities between our findings, including key predictors of angle widening after LPI, and  
342 findings in data from South Indian eyes.<sup>6</sup> Finally, the R-squared metrics of our multivariable models were  
343 poor. Therefore, further work is required to identify more predictive parameters before statistical models  
344 can be used to predict precisely how a patient will or will not benefit from LPI.

345 In conclusion, we characterized and modeled LPI-related anatomical changes in Chinese subjects  
346 with PACS. Our key finding is that a superiorly placed LPI results in greater angle widening on average  
347 and lower odds of poor angle widening compared a temporally or nasally placed LPI. Based on these  
348 results, eyecare providers may consider a superior LPI location to optimize anatomical changes after LPI.  
349 However, the long-term clinical implications of this additional angle widening and the mechanism that  
350 underlies this effect remain unclear. This approach may also predispose patients to a higher risk of  
351 dysphotopsias.<sup>11-13</sup> We hope this study inspires additional research to improve the effectiveness of LPI for  
352 widening the angle and reducing the risk of PACG in angle closure eyes.

353

#### 354 **Acknowledgements**

355 This work was supported by grants K23 EY029763 and P30 EY029220 from the National Eye Institute,  
356 National Institute of Health, Bethesda, Maryland; a Young Clinician Scientist Research Award from the  
357 American Glaucoma Society; and an unrestricted grant to the Department of Ophthalmology from  
358 Research to Prevent Blindness, New York, NY. The ZAP Trial was supported by the Fight for Sight  
359 (grant 1655; UK), the Sun Yat-sen University 5010 Project Fund (grant 2007033; China), the National  
360 Natural Science Foundation of China (grant 81420108008; China), Fundamental Research Funds of the  
361 State Key Laboratory in Ophthalmology (China), and Moorfields Eye Charity (previously Special  
362 Trustees of Moorfields Eye Hospital).

363

364 **References**

- 365 1. Quigley H, Broman AT. The number of people with glaucoma worldwide in 2010 and 2020. *Br J*  
366 *Ophthalmol.* 2006;90(3):262-267.
- 367 2. Tham YC, Li X, Wong TY, Quigley HA, Aung T, Cheng CY. Global prevalence of glaucoma and  
368 projections of glaucoma burden through 2040: A systematic review and meta-analysis.  
369 *Ophthalmology.* 2014;121(11):2081-2090.
- 370 3. Weinreb RN, Aung T, Medeiros FA. The pathophysiology and treatment of glaucoma: A review.  
371 *JAMA - J Am Med Assoc.* 2014;311(18):1901-1911.
- 372 4. Azuara-Blanco A, Burr J, Ramsay C, et al. Effectiveness of early lens extraction for the treatment  
373 of primary angle-closure glaucoma (EAGLE): a randomised controlled trial. *Lancet.*  
374 2016;388(10052):1389-1397.
- 375 5. Radhakrishnan S, Chen PP, Junk AK, Nouri-Mahdavi K, Chen TC. Laser Peripheral Iridotomy in  
376 Primary Angle Closure. *Ophthalmology.* 2018;125(7):1110-1120.
- 377 6. Zebardast N, Kavitha S, Krishnamurthy P, et al. Changes in Anterior Segment Morphology and  
378 Predictors of Angle Widening after Laser Iridotomy in South Indian Eyes. *Ophthalmology.*  
379 2016;123(12):2519-2526.
- 380 7. How AC, Baskaran M, Kumar RS, et al. Changes in anterior segment morphology after laser  
381 peripheral iridotomy: An anterior segment optical coherence tomography study. *Ophthalmology.*  
382 2012;119(7):1383-1387.
- 383 8. Lee RY, Kasuga T, Cui QN, Huang G, He M, Lin SC. Association between baseline angle width  
384 and induced angle opening following prophylactic laser peripheral iridotomy. *Invest Ophthalmol*  
385 *Vis Sci.* 2013;54(5):3763-3770.
- 386 9. Huang G, Gonzalez E, Lee R, et al. Anatomic predictors for anterior chamber angle opening after  
387 laser peripheral iridotomy in narrow angle eyes. *Curr Eye Res.* 2012;37(7):575-582.
- 388 10. Sidhartha E, Gupta P, Liao J, et al. Assessment of iris surface features and their relationship with



- 389 iris thickness in Asian eyes. *Ophthalmology*. 2014;121(5):1007-1012.
- 390 11. Vera V, Naqi A, Belovay GW, Varma DK, Ahmed IIK. Dysphotopsia after temporal versus  
391 superior laser peripheral iridotomy: A prospective randomized paired eye trial. *Am J Ophthalmol*.  
392 2014;157(5).
- 393 12. Srinivasan K, Zebardast N, Krishnamurthy P, et al. Comparison of New Visual Disturbances after  
394 Superior versus Nasal/Temporal Laser Peripheral Iridotomy: A Prospective Randomized Trial.  
395 *Ophthalmology*. 2018;125(3):345-351.
- 396 13. Congdon N, Yan X, Friedman DS, et al. Visual symptoms and retinal straylight after laser  
397 peripheral iridotomy: The zhongshan angle-closure prevention trial. *Ophthalmology*.  
398 2012;119(7):1375-1382.
- 399 14. He M, Jiang Y, Huang S, et al. Laser peripheral iridotomy for the prevention of angle closure: a  
400 single-centre, randomised controlled trial. *Lancet*. 2019;393(10181):1609-1618.
- 401 15. Jiang Y, Friedman DS, He M, Huang S, Kong X, Foster PJ. Design and methodology of a  
402 randomized controlled trial of laser iridotomy for the prevention of angle closure in Southern  
403 China: The zhongshan angle closure prevention trial. *Ophthalmic Epidemiol*. 2010;17(5):321-332.
- 404 16. Console JW, Sakata LM, Aung T, Friedman DS, He M. Quantitative analysis of anterior segment  
405 optical coherence tomography images: The zhongshan angle assessment program. *Br J*  
406 *Ophthalmol*. 2008;92(12):1612-1616.
- 407 17. Ho SW, Baskaran M, Zheng C, et al. Swept source optical coherence tomography measurement of  
408 the iris-trabecular contact (ITC) index: A new parameter for angle closure. *Graefe's Arch Clin Exp*  
409 *Ophthalmol*. 2013;251(4):1205-1211.
- 410 18. Leung CKS, Weinreb RN. Anterior chamber angle imaging with optical coherence tomography.  
411 *Eye*. 2011;25(3):261-267.
- 412 19. Mansouri M, Ramezani F, Moghimi S, et al. Anterior segment optical coherence tomography  
413 parameters in phacomorphic angle closure and mature cataracts. *Investig Ophthalmol Vis Sci*.  
414 2014;55(11):7403-7409.

- 415 20. Narayanaswamy A, Sakata LM, He MG, et al. Diagnostic performance of anterior chamber angle  
416 measurements for detecting eyes with narrow angles: An anterior segment OCT study. *Arch*  
417 *Ophthalmol.* 2010;128(10):1321-1327.
- 418 21. Tun TA, Baskaran M, Perera SA, et al. Sectoral variations of iridocorneal angle width and iris  
419 volume in Chinese Singaporeans: A swept-source optical coherence tomography study. *Graefe's*  
420 *Arch Clin Exp Ophthalmol.* 2014;252(7):1127-1132.
- 421 22. Xu BY, Israelsen P, Pan BX, Wang D, Jiang X, Varma R. Benefit of measuring anterior segment  
422 structures using an increased number of optical coherence tomography images: The Chinese  
423 American Eye Study. *Investig Ophthalmol Vis Sci.* 2016;57(14):6313-6319.
- 424 23. Lee RY, Kasuga T, Cui QN, Huang G, He M, Lin SC. Comparison of anterior segment  
425 morphology following prophylactic laser peripheral iridotomy in Caucasian and Chinese eyes.  
426 *Clin Exp Ophthalmol.* 2014;42(5):417-426.
- 427 24. Zheng C, Guzman CP, Cheung CY, et al. Analysis of anterior segment dynamics using anterior  
428 segment optical coherence tomography before and after laser peripheral iridotomy. *Arch*  
429 *Ophthalmol.* 2013;131(1):44-49.
- 430 25. Huang G, Gonzalez E, Lee R, Chen YC, He M, Lin SC. Association of biometric factors with  
431 anterior chamber angle widening and intraocular pressure reduction after uneventful  
432 phacoemulsification for cataract. *J Cataract Refract Surg.* 2012;38(1):108-116.
- 433 26. Moghimi S, Chen R, Hamzeh N, Khatibi N, Lin SC. Qualitative evaluation of anterior segment in  
434 angle closure disease using anterior segment optical coherence tomography. *J Curr Ophthalmol.*  
435 2016;28(4):170-175.
- 436 27. Leung CKS, Cheung CYL, Li H, et al. Dynamic analysis of dark-light changes of the anterior  
437 chamber angle with anterior segment OCT. *Investig Ophthalmol Vis Sci.* 2007;48(9):4116-4122.
- 438 28. Xu BY, Lifton J, Burkemper B, et al. Ocular Biometric Determinants of Anterior Chamber Angle  
439 Width in Chinese Americans: The Chinese American Eye Study. *Am J Ophthalmol.* 2020;220.
- 440 29. Foster PJ, Buhrmann R, Quigley HA, Johnson GJ. The definition and classification of glaucoma in

- 441 prevalence surveys. *Br J Ophthalmol.* 2002;86(2):238-242.
- 442 30. Porporato N, Baskaran M, Tun TA, et al. Understanding diagnostic disagreement in angle closure  
443 assessment between anterior segment optical coherence tomography and gonioscopy. *Br J*  
444 *Ophthalmol.* 2019;104(6).
- 445 31. Xu BY, Pardeshi AA, Burkemper B, et al. Differences in Anterior Chamber Angle Assessments  
446 Between Gonioscopy, EyeCam, and Anterior Segment OCT: The Chinese American Eye Study.  
447 *Transl Vis Sci Technol.* 2019;8(2):5.

448

**449 Table Captions**

450 **Table 1.** Mean parameter measurements at baseline and 2 weeks after LPI and change in mean parameter  
451 measurements after LPI.

452 **Table 2.** Univariable and multivariable linear regression analysis of the relationship between baseline  
453 parameters and change in mean AOD750 after LPI adjusted for age and sex.

454 **Table 3.** Multivariable logistic regression model with significant baseline predictors of poor angle  
455 widening (lowest quintile of change in AOD750) after LPI adjusted for age and sex.

456 **Table 4.** Multivariable logistic regression model with significant baseline predictors of poor angle  
457 opening (residual PACS) after LPI adjusted for age and sex.

458 **Table 5.** Mean parameter measurements at baseline by LPI location.

459

**Table 1:** Mean parameter measurements at baseline and 2 weeks after LPI and change in mean parameter measurements after LPI.

Parameter	Baseline Before LPI		2 Weeks After LPI		P-value *	Change After LPI	
	Mean	STD	Mean	STD		Mean	STD
AOD500, mm	0.082	0.044	0.136	0.055	<b>&lt;0.001</b>	0.054	0.042
AOD750, mm	0.127	0.058	0.206	0.071	<b>&lt;0.001</b>	0.079	0.052
TISA500, mm <sup>2</sup>	0.041	0.020	0.059	0.024	<b>&lt;0.001</b>	0.018	0.016
TISA750, mm <sup>2</sup>	0.074	0.030	0.110	0.036	<b>&lt;0.001</b>	0.036	0.025
IT750, mm	0.496	0.061	0.499	0.060	<b>0.006</b>	0.004	0.034
IT2000, mm	0.640	0.059	0.637	0.059	0.114	-0.003	0.039
IA, mm <sup>2</sup>	1.625	0.196	1.607	0.200	<b>&lt;0.001</b>	-0.017	0.104
IC, mm <sup>2</sup>	0.355	0.078	0.199	0.084	<b>&lt;0.001</b>	-0.157	0.098
ACD, mm	2.227	0.197	2.236	0.197	<b>&lt;0.001</b>	0.009	0.022
ACW, mm	11.640	0.365	11.681	0.363	<b>&lt;0.001</b>	0.040	0.140
ACA, mm <sup>2</sup>	15.938	1.992	16.723	1.891	<b>&lt;0.001</b>	0.786	0.441
LV, mm	0.760	0.177	0.782	0.180	<b>&lt;0.001</b>	0.022	0.068
PD, mm	4.528	0.753	4.404	0.835	<b>&lt;0.001</b>	-0.121	0.691

Abbreviations: AOD500/750: Angle opening distance 500/750 um from the scleral spur. TISA500/750: Trabecular-iris space area 500/750 um from the scleral spur. IT750/2000: Iris Thickness 750/2000 um from the scleral spur. IA: Iris Area. IC: Iris Curvature. ACD: Anterior Chamber Depth. ACW: Anterior Chamber Width. ACA: Anterior Chamber Area. LV: Lens Vault. PD: Pupillary Diameter.

\* P-values calculated using Wilcoxon signed-rank test.

Boldface indicated significant at  $P < 0.05$ .

**Table 2:** Univariable and multivariable linear regression analysis of the relationship between baseline parameters and change in mean AOD750 after LPI adjusted for age and sex.

Parameter	Interval	Univariable *		Multivariable * <sup>b</sup>	
		Change in AOD750 (um)	P-value	Change in AOD750 (um)	P-value
Age	Years	0.573	0.288 <sup>a</sup>		
Sex	Female	-0.447	0.948 <sup>a</sup>		
Mean gonioscopy grade	1 mShaffer grade	7.1677	0.306		
LPI location	Temporal/Nasal	<b>-11.087</b>	<b>0.025</b>	<b>-12.809</b>	<b>0.004</b>
AOD500	0.1 mm	-4.552	0.423		
AOD750	0.1 mm	<b>-16.978</b>	<b>&lt;0.001</b>	<b>-20.806</b>	<b>&lt;0.001</b>
TISA500	0.1 mm <sup>2</sup>	-2.682	0.832		
TISA750	0.1 mm <sup>2</sup>	-8.142	0.328		
IT750	0.1 mm	<b>-13.150</b>	<b>0.001</b>		
IT2000	0.1 mm	-6.223	0.142		
IA	0.1 mm <sup>2</sup>	0.669	0.597	<b>-6.546</b>	<b>&lt;0.001</b>
IC	0.1 mm	<b>19.360</b>	<b>&lt;0.001</b>	<b>18.178</b>	<b>&lt;0.001</b>
ACD	0.1 mm	<b>-3.238</b>	<b>0.010</b>	<b>3.849</b>	<b>0.010</b>
ACW	1 mm	-9.221	0.173		
ACA	1 mm <sup>2</sup>	<b>-4.364</b>	<b>&lt;0.001</b>		
LV	0.1 mm	<b>4.622</b>	<b>0.001</b>		
PD	0.1 mm	<b>-1.199</b>	<b>&lt;0.001</b>	<b>-2.332</b>	<b>&lt;0.001</b>
ΔPD	0.1 mm	<b>-1.242</b>	<b>0.001</b>	<b>-1.720</b>	<b>&lt;0.001</b>

**Abbreviations:** AOD500/750: Angle opening distance 500/750 um from the scleral spur. TISA500/750: Trabecular-iris space area 500/750 um from the scleral spur. IT750/2000: Iris Thickness 750/2000 um from the scleral spur. IA: Iris Area. IC: Iris Curvature. ACD: Anterior Chamber Depth. ACW: Anterior Chamber Width. ACA: Anterior Chamber Area. LV: Lens Vault. PD: Pupillary Diameter. ΔPD: Change in PD after LPI.

\* P-values calculated using age- and sex-adjusted linear regressions.

<sup>a</sup> Univariable models of sex and age adjusted for age and sex, respectively.

<sup>b</sup> Variance inflation factor (VIF) < 1.75 for all parameters.

Boldface indicated significant at P < 0.05.

**Table 3.** Multivariable logistic regression model with significant baseline predictors of poor angle widening (lowest quintile of change in AOD750) after LPI adjusted for age and sex.

Parameter	Interval	Multivariable *		
		OR	95% CI	P-value
LPI location	Temporal/Nasal	2.597	1.541 - 4.470	<0.001
AOD750	0.1 mm	2.583	1.507 - 4.538	<0.001
IA	0.1 mm <sup>2</sup>	1.351	1.127 - 1.628	<0.001
IC	0.1 mm	0.395	0.262 - 0.579	<0.001
PD	0.1 mm	1.125	1.070 - 1.188	<0.001
ΔPD	0.1 mm	1.060	1.014 - 1.112	0.013

Abbreviations: AOD500/750: Angle opening distance 500/750 um from the scleral spur. TISA500/750: Trabecular-iris space area 500/750 um from the scleral spur. IT750/2000: Iris Thickness 750/2000 um from the scleral spur. IA: Iris Area. IC: Iris Curvature. ACD: Anterior Chamber Depth. ACW: Anterior Chamber Width. ACA: Anterior Chamber Area. LV: Lens Vault. PD: Pupillary Diameter. ΔPD: Change in PD after LPI.

\* P-values calculated using age- and sex-adjusted linear regressions. Variance inflation factor (VIF) < 1.94 for all parameters.

**Table 4.** Multivariable logistic regression model with significant baseline predictors of poor angle opening (residual PACS) after LPI adjusted for age and sex.

Parameter	Interval	Multivariable *		
		OR	95% CI	P-value
IA	0.1 mm <sup>2</sup>	1.209	1.056 - 1.388	0.006
IC	0.1 mm	0.539	0.389 - 0.732	<0.001
Mean gonioscopy grade	1 mShaffer grade wider	0.335	0.175 - 0.632	0.001

Abbreviations: IA: Iris Area. IC: Iris Curvature.

\* P-values calculated using age- and sex-adjusted linear regressions. Variance inflation factor (VIF) < 1.49 for all parameters.

**Table 5:** Mean parameter measurements at baseline stratified by LPI location.

Parameter	Superior (N = 219)		Temporal/Nasal (N = 235)		P-value *
	Mean	STD	Mean	STD	
Age, years	57.991	4.789	58.319	4.586	0.476
Sex (M/F)	33	186	40	195	0.571 <sup>a</sup>
AOD500, mm	0.084	0.044	0.080	0.044	0.387
AOD750, mm	0.129	0.055	0.125	0.060	0.282
TISA500, mm <sup>2</sup>	0.041	0.020	0.042	0.019	0.765
TISA750, mm <sup>2</sup>	0.075	0.030	0.074	0.030	0.865
IT750, mm	0.481	0.063	0.487	0.071	0.723
IT2000, mm	0.495	0.064	0.498	0.058	0.983
IA, mm <sup>2</sup>	0.638	0.056	0.641	0.062	0.514
IC, mm <sup>2</sup>	1.618	0.197	1.631	0.195	0.973
ACD, mm	2.247	0.191	2.208	0.202	<b>0.024</b>
ACW, mm	11.659	0.344	11.622	0.384	0.199
ACA, mm <sup>2</sup>	16.139	1.960	15.751	2.008	<b>0.039</b>
LV, mm	0.754	0.165	0.765	0.187	0.793
PD, mm	4.601	0.735	4.460	0.765	0.065

Abbreviations: AOD500/750: Angle opening distance 500/750 um from the scleral spur. TISA500/750: Trabecular-iris space area 500/750 um from the scleral spur. IT750/2000: Iris Thickness 750/2000 um from the scleral spur. IA: Iris Area. IC: Iris Curvature. ACD: Anterior Chamber Depth. ACW: Anterior Chamber Width. ACA: Anterior Chamber Area. LV: Lens Vault. PD: Pupillary Diameter.

\* P-values calculated using age- and sex-adjusted linear regressions.

<sup>a</sup> P-value calculated using chi-square test.

Boldface indicated significant at  $P < 0.05$ .



**Précis**

Laser peripheral iridotomy in Chinese primary angle closure suspects produces angle widening on anterior segment OCT and opening on gonioscopy. Superior laser locations result in greater angle widening compared to temporal or nasal locations.

Journal Pre-proof